Conventional and Air-breathing Electric Propulsion Trade-offs for VLEO Nanosatellites

IEPC-2025-282

Presented at the 39th International Electric Propulsion Conference
Imperial College London • London, United Kingdom
14-19 September 2025

Eugenio Ferrato[1*], Bruno Moriconi[2*], Thomas Gerard[3*], Vittorio Giannetti[4*], and Tommaso Andreussi[5*]
[*]*Sant'Anna School of Advanced Studies, Pisa, 56127, Italy*

Abstract: Very Low Earth Orbit (VLEO) offers unique opportunities for satellite missions, including higher spatial resolution, reduced communication latency, and improved link budget. Yet, the persistence of aerodynamic drag at these altitudes makes orbit maintenance particularly challenging, especially for CubeSat-class platforms where mass, volume, and power limitations restrict the operational capability of conventional propulsion. This work investigates the integration of air-breathing electric propulsion (ABEP) as an alternative to propellant-based systems, with the aim of identifying mission and propulsion requirements that enable sustainable operations in VLEO. A comparative trade-off between ABEP and conventional solutions is performed for a reference 6U nanosatellite platform, highlighting the efficiency, lifetime, and feasibility thresholds that must be met to unlock future nanosatellite-based VLEO missions.

I. Introduction

VERY Low Earth Orbit (VLEO) offers unique opportunities for satellite missions. Proximity to Earth's surface enhances communication capabilities by reducing latency and transmission power while maintaining data link performance [1]. For Earth observation, VLEO improves imaging conditions, enabling higher-resolution reconnaissance. Additionally, the reduced altitude allows for enhanced payload performance, potentially minimizing satellite platform size [2-3]. Operating in the upper atmosphere further reduces exposure to radiation [4] while mitigating the challenge of space debris [5]. However, the atmospheric environment at these altitudes poses significant challenges, particularly in sustaining the orbit for meaningful mission durations due to continuous aerodynamic drag. This issue is especially critical for CubeSat-class platforms, where mass, volume, and power constraints limit the feasibility of traditional propulsion methods [6].

In this context, the concept of air-breathing electric propulsion (ABEP) represents a potential enabling technology for sustained VLEO spaceflight [7]. ABEP relies on an intake placed in front of the spacecraft to gather the same atmospheric particles that generate the drag. Utilizing electric power derived from solar arrays or batteries, an electric thruster then ionizes and accelerates these particles to generate thrust. By leveraging these limited yet renewable resources, it becomes possible to decouple the spacecraft's lifetime from the availability of propellant, enabling extended mission durations at low altitudes. However, ABEP implementation involves complex trade-offs. Below a critical altitude, excessive power is required to process the collected flow, while at higher altitudes the low density of rarefied particles limits ionization and thus thrust generation [6], In addition, the feasibility of air-breathing platforms depends not only on aerodynamics, power generation capabilities, and thrust generation efficiency, but also on the practical realization of GNC schemes for robust altitude maintenance, which remains a non-trivial challenge [8-9].

[1] Assistant Professor, Institute of Mechanical Intelligence, eugenio.ferrato@santannapisa.it
[2] PhD Student, Institute of Mechanical Intelligence, bruno.moriconi@santannapisa.it
[3] Research Fellow, Institute of Mechanical Intelligence, thomas.gerard@santannapisa.it
[4] Assistant Professor, Institute of Mechanical Intelligence, vittorio.giannetti@santannapisa.it
[5] Full Professor, Institute of Mechanical Intelligence, tommaso.andreussi@santannapisa.it

This naturally raises the question of how competitive ABEP can truly be compared to conventional propulsion solutions for nanosatellites that are already available on the market. To address this question, this study investigates the feasibility requirements of air-breathing electric propulsion (ABEP) systems compared to conventional propellant-based solutions, using a reference 6U CubeSat platform. This work has been carried out within the framework of the ARIA project, funded by the Italian Ministry of University and Research, which aims to demonstrate the feasibility of the ABEP concept and pave the way for its application on nanosatellite platforms. Project activities are focused on: i) defining mission scenarios and platform designs for CubeSats embarking the ABEP technology ii) realizing a wind tunnel to provide a controlled environment for prototype testing; iii) identifying the optimal ABEP design for the selected platform architecture and system requirements.

In Section II, a systematic trade-off analysis is performed across multiple orbit and platform configurations to derive representative values of drag, solar power availability, and propulsion power allocation. Based on these results, Section III discusses the efficiency, lifetime, and feasibility thresholds, with the goal of identifying the conditions under which ABEP can offer a tangible advantage over conventional systems. In doing so, this work is intended to provide a preliminary reference for CubeSat mission design in VLEO, outlining first-iteration requirements that may inform the development of future nanosatellite-based missions in the VLEO orbital regime.

II.Mission and Platform Architecture Tradeoffs

A. Application Orbits

To serve as a reference for this study, a review of existing and upcoming satellite constellations application orbits is provided in Table 1. Earth observation constellations typically make use of sun-synchronous orbits, thanks to the repeatability of illumination conditions and global coverage even at high latitudes. On the other hand, telecommunications constellations typically utilize inclined circular orbits to optimize coverage and minimize the number of satellites required to meet specific revisit time requirements, as the majority of Earth's population resides below 60° latitude.

Table 1. Application orbit for some existing of upcoming constellations.

Use case	Constellation Name	Orbit Parameters	Ref
Telecom	Starlink	340-630 km, 43°-97.6°	[10]
Telecom	OneWeb	1200 km, 40-87.9°	[10]
Telecom	TeleSat	1015-1325 km, 50.9°-98.9°	[10]
Telecom	Amazon	590-630 km, 33°-51.9°	[10]
Earth Observation	PlanetScope	475-525 km, SSO 9:30-11:30 am	[11]
Earth Observation	ICEEYE	560-580 km, SSO 2-3 pm	[12]
Earth Observation	WorldView	617-681 km, SSO 10:30 am	[13]

Consistently with Table 1, a set of 24 circular orbits are here investigated as possible destination orbits for air-breathing satellites, see Figure 1. These include sun-synchronous orbits with local times of ascending node at 6:00 AM, 10:00 AM, and 2:00 PM at mean altitudes of 250 km and 300 km. Additionally, inclined orbits with inclinations of 75°, 67.5°, and 45° are considered at right ascension of ascending nodes (RAAN) of 0°, 120°, and 240°, also at altitudes of 250 km and 300 km. Each orbit presents specific demands on the ABEP system, including an average thrust requirement and corresponding power consumption.

These requirements are influenced by the mean atmospheric flow density at the orbit, as well as factors such as eclipse durations and the relative position of the Sun to the spacecraft's solar arrays, which impact solar power generation. For the purpose of the present analysis, each orbit is identified with an identification number as reported in Table 2

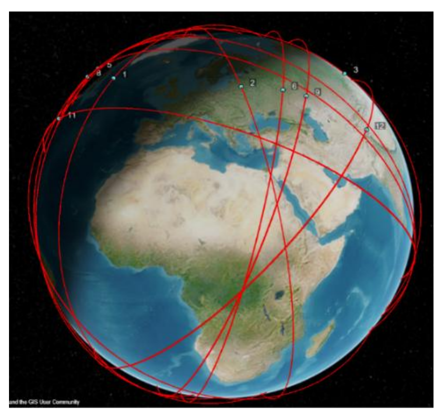

Figure 1. Illustration of 250 km of altitude sun-synchronous and inclined circular orbits, identified as per Table 2.

Table 2. Definition of reference application orbits selected for the present analysis. RAAN for SSO orbits has been computed by selecting 1stJanuary 2021 midnight as reference time.

Orbit ID	h [km]	a [km]	e	i [deg]	RAAN [deg]	Notes
1	250	6628.14	0	96.4784	190.86471	SSO 6:00 am
2	250	6628.14	0	96.4784	250.86471	SSO 10:00 am
3	250	6628.14	0	96.4784	310.86471	SSO 2:00 pm
4	250	6628.14	0	75	0	
5	250	6628.14	0	75	120	
6	250	6628.14	0	75	240	
7	250	6628.14	0	67.5	0	
8	250	6628.14	0	67.5	120	
9	250	6628.14	0	67.5	240	
10	250	6628.14	0	45	0	
11	250	6628.14	0	45	120	
12	250	6628.14	0	45	240	
13	300	6678.14	0	96.6522	190.86471	SSO 6:00 am
14	300	6678.14	0	96.6522	250.86471	SSO 10:00 am
15	300	6678.14	0	96.6522	310.86471	SSO 2:00 pm
16	300	6678.14	0	75	0	
17	300	6678.14	0	75	120	
18	300	6678.14	0	75	240	
19	300	6678.14	0	67.5	0	
20	300	6678.14	0	67.5	120	
21	300	6678.14	0	67.5	240	
22	300	6678.14	0	45	0	
23	300	6678.14	0	45	120	
24	300	6678.14	0	45	240	

B. Overview of Platform Configurations

In general, a VLEO platform should minimize drag while maximizing the solar power available. For an air-breathing platform, also the collection of atmospheric particles should be optimized. Accordingly, nominal spacecraft configurations with fixed solar arrays aligned with the flow direction are considered for drag minimization. This approach eliminates the need for a Solar Array Drive Assembly (SADA) mechanism, which may significantly reduce the mean solar power available depending on the orbit. To optimize propellant collection, the spacecraft's nominal orientation should be maintained in alignment with the Velocity-Normal-Binormal (VNB) frame, ensuring that the intake axis is well-aligned with the orbital velocity direction.

The main trade-offs in platform architecture focus on the arrangement of the solar arrays and the orientation of the platform body relative to the orbital velocity. Different configurations are defined by the hinge position and relative orientation of the two solar panels, as well as the number of deployable array folds. For this analysis, the three-folds GomSpace deployable solar array TSP-45W is chosen as a reference [14], with each deployed 3-folds panel measuring 208 mm x 930 mm and providing 45 W of power in fully illuminated condition (i.e., ~250 W/m2). In configurations with one or two folds, performance is assumed to scale proportionally. Regarding the platform body orientation, a 2U form factor is assumed for the air-breathing propulsion subsystem so to minimize the volume occupied by the ABEP system. All configurations are thus aligned with the side of the 2U length facing the velocity direction, resulting in a frontal area of 0.03 m².

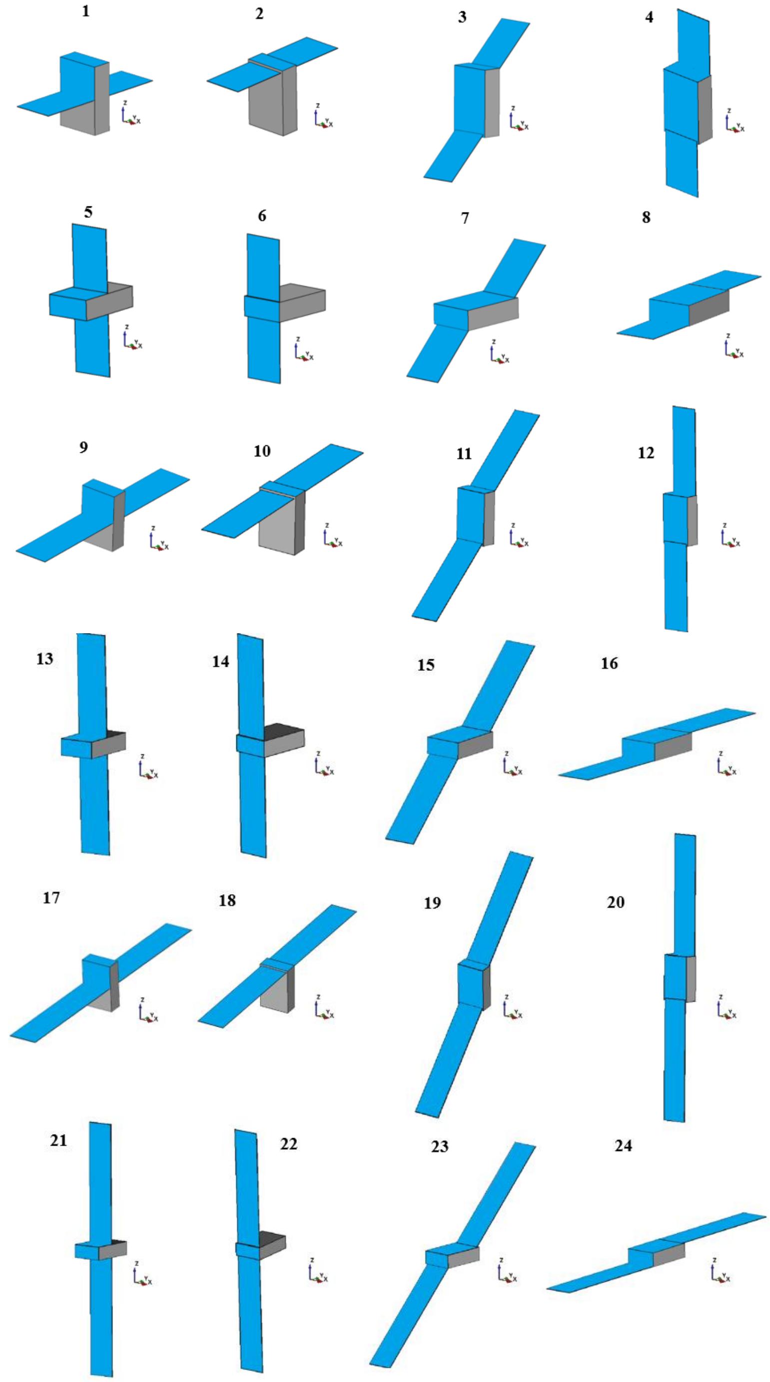

Figure 2. Investigated platform configurations. Blue-shaded area represents surfaces for solar energy generation. The nominal flight direction is directed along the x body axis.

Figure 2 presents the 24 platform configurations examined in this study, with the shaded blue area highlighting the portion of the platform surface covered by solar cells. Table 3 provides the corresponding power-generating surface area for each configuration, specifying values for solar cell orientations with the normal aligned along the platform's y-axis, z-axis, and at a 45° angle. Along with the frontal drag area A_f for each configuration, these parameters are employed for the subsequent trade-off analysis.

Table 3. Drag and solar cells surface area for the investigated platform configurations. Each platform is numbered consistently with Figure 2.

Platform ID	A_f [m^2]	A_y [m^2]	A_z [m^2]	A_{45} [m^2]
1	0.03	0.03	0.14	0
2	0.03	0	0.14	0
3	0.03	0.06	0.02	0.12
4	0.03	0.18	0.02	0
5	0.03	0.14	0.03	0
6	0.03	0.14	0	0
7	0.03	0.02	0.06	0.12
8	0.03	0.02	0.18	0
9	0.03	0.03	0.26	0
10	0.03	0	0.26	0
11	0.03	0.06	0.02	0.24
12	0.03	0.3	0.02	0
13	0.03	0.26	0.03	0
14	0.03	0.26	0	0
15	0.03	0.02	0.06	0.24
16	0.03	0.02	0.3	0
17	0.03	0.03	0.38	0
18	0.03	0	0.38	0
19	0.03	0.06	0.02	0.36
20	0.03	0.42	0.02	0
21	0.03	0.38	0.03	0
22	0.03	0.38	0	0
23	0.03	0.02	0.06	0.36
24	0.03	0.02	0.42	0

C. COTS Subsystems Selection and Propulsion Integration

Building on the target mission objectives, a set of reference platform subsystems have been identified. Components from GomSpace [15] have been adopted as references for most units, primarily due to the availability of comprehensive documentation and flight-proven heritage. Leveraging its extensive flight heritage, the commercial off-the-shelf SimeraSense TriScape 100 camera [16] is adopted as a reference payload. According to its datasheet, it delivers 4.75 m ground sampling distance (GSD) at 500 km, improving to 2.375 m at 250 km that would be an exceptional capability for a 6U CubeSat. While specifications may differ across suppliers, CubeSat subsystems generally exhibit broadly comparable characteristics, making this baseline suitable for preliminary sizing the air-breathing platform.

The list of selected COTS units and reference datasheet is provided in Table 4, together with the main technical budgets of the selected platform components except propulsion.

Table 4. Reference COTS CubeSat Units Technical Budgets.

Subsys.	Component	Units	Unit Mass [kg]	Unit Volume [dm^3]	Unit Mean Power [W]	Unit Peak Power [W]	Notes
Payload	Triscape 100 camera [16]	1	1.26	1.7	2.7*	6.75	*Idle power
Power	Solar arrays TSP-45W [14]	2	0.75*	-	-	-	*3 folds SA
	86 Wh Battery BPX [18]	1	0.5	0.32	-	-	
	PDU NanoPower P60 [19]	1	0.62	0.587	1.25	1.25	
Attitude	Twinkle Star Tracker [22]	2	0.035	0.1	0.5	0.5	
	4 reaction wheels ass. NanoTorque GSW-600 [20]	1	0.94	0.56	1.2	10	
	NovAtel OEM719 GPS receiver [24]	1	0.032	0.036	1.32	1.32	
	NanoSense M315 Magnetometer [23]	2	0.008	0.004	0.008	0.008	
	GST-600 3-axis Magnetorquer [21]	1	0.156	0.150	0.3	5	typical, peak up to 5 W
Telecom	S-band transceiver NanoCom Link S [26] and antenna ANT2150 [27]	1	0.395	0.409	0.17*	24	0.25 Wh per orbit for an assumed 10 min passes per day at peak power.
Comm. & Data	On-board Computer NanoMind HPMK3 [25]	1	0.024	0.018	0.17*	1	*typical power
Struc.	6U Structure	1	1.060	-	-	-	
	TOTAL w/o margins		**6.57**	**3.988**	**8.17**	**50.33**	

Based on the preliminary power budget, the platform is expected to supply an average power of approximately $P_{SS} = 5.5$ W to its subsystems, in addition to a mean power level of P_{PL}=2.7 W allocated to the payload. Regarding the volume allocation and ABEP integration, the preliminary volume budget indicates the feasibility of dedicating 2U to the air-breathing propulsion subsystem. An example of physical architecture of the air-breathing nanosatellite is illustrated in Figure 3.

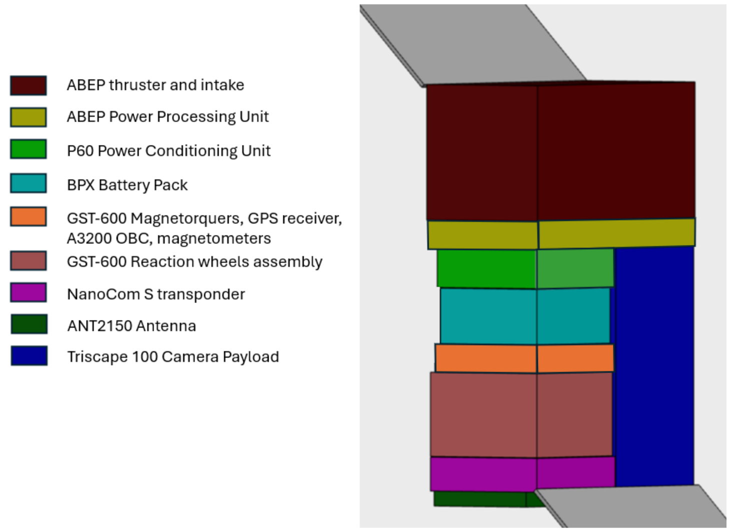

Figure 3. Example of physical architecture for a 6U air-breathing nanosatellite.

D. Tradeoff Criteria

The goal of the trade-off is to identify the optimal combination of application orbit and platform configuration that minimizes the performance requirements for the air-breathing thruster, while ensuring drag compensation and adherence to the platform's power budget within the 250 km to 300 km altitude range, proceeding then toward a quantitative comparison with existing COTS propulsion solutions.

Considering orbit-averaged properties, to fully compensate for drag the propulsion subsystem should be capable of producing a mean thrust T of at least

$$T > D/\delta_{EP}, \tag{1}$$

where D is the drag acting on the whole platform and δ_{EP} is the thruster duty cycle. The mean electric propulsion power consumption will then be equal to

$$P_{EP} = \frac{T I_{sp} g_0}{2\eta_T} \tag{2}$$

where η_T is the thrust efficiency

For air-breathing systems, considering the intake-thruster coupling resulting in a given collection efficiency η_C and pressure ratio r, to fully compensate the drag the thruster shall be capable of producing a minimum specific impulse of

$$I_{sp} > \frac{D}{\delta_{EP}\rho_\infty u_\infty A_{itk}\eta_c g_0} \tag{3}$$

where ρ_∞ and u_∞ are the mean atmospheric mass density and orbital velocity associated with a given orbit, g_0 is Earth's gravity at sea level, η_c is the intake collection efficiency, and A_{itk} is the intake inlet area, set equal to 0.01 m^2 as per the CubeSat physical architecture preliminarily defined in Figure 3. Combining the three equations above, we can see how for ABEP system the orbit-average energy consumption E_{EP} results in

$$E_{EP} \propto P_{EP}\delta_{EP} = \frac{D^2}{2\delta_{EP}\rho_\infty u_\infty A_{itk}\eta_c\eta_t} \tag{4}$$

which scales inversely with the ABEP duty cycle. As a result, continuous drag compensation ($\delta_{EP} = 1$) offers the highest energy efficiency for ABEP systems, whereas in conventional propulsion the duty cycle does not affect the average energy consumption per orbit.

For both conventional and air-breathing systems, compliance to the orbit-average energy balance can then be expressed by the requirement

$$P_{av} \geq \delta_{EP} P_{EP} + P_{SS} + \delta_{PL} P_{PL} + \frac{\alpha}{1-\alpha} P_{ecl} \quad (5)$$

where P_{av} is the orbit-averaged power produced by solar arrays when the spacecraft is illuminated, δ_{PL} is the payload duty cycle, and the fourth right-hand term of equation above represents the fraction of power to be allocated for battery recharging, being α the mean eclipse duration to orbital period ratio. In this regard, different concepts of operation may be identified. These are determined by factors such as whether the propulsion system can function during payload acquisition or data transmission (e.g., due to electromagnetic compatibility constraints), whether propulsion is active during eclipse periods, and whether the payload must also operate during eclipses.

For the purpose of the present analysis, the following simplifications and assumptions will be made:

- The ABEP propulsion subsystem is assumed to operate continuously, even in eclipse periods;
- The payload is assumed to operate continuously at idle power, resulting in a mean power consumption of 4 Wh per orbit according to the power budget outlined in Table 4.
- All the other platform subsystem are assumed to operate continuously at a mean power level outlined in Table 4, resulting in a mean power consumption of 8.25 Wh per orbit.

By considering $P_{ecl} = P_{EP} + P_{SS} + P_{PL}$ consistently with the assumptions above, the mean power that can be allocated to the EP system follows from Eq. 5 as

$$P_{EP} \leq (1-\alpha) P_{av} - P_{SS} - P_{PL} \quad (6)$$

Which can be translated into a conventional EP efficiency requirement

$$\eta_T \geq \frac{D I_{sp} g_0}{2 P_{EP}} \quad (7)$$

and an equivalent ABEP efficiency requirement

$$\eta_c \eta_T \geq \frac{D^2}{2 \rho_\infty u_\infty A_{itk} P_{EP}} \quad (8)$$

Accordingly, for each of the investigated orbit/platform combination, the objective of the present trade-off is to:

- Define the key requirements for the ABEP system, expressed in terms of combined collection and thrust efficiencies ($\eta_C \eta_T$);
- Define the key requirements for a conventional propulsion system, expressed in terms of thrust efficiency (η_T);
- Compare the minimum operational lifetime that ABEP must demonstrate in order to deliver greater total impulse than state-of-the-art conventional propulsion;
- Verify that mean aerodynamic torques remain within the control authority of the selected magnetorquers, thereby preventing long-term reaction wheel saturation and ensuring robust attitude control;
- Identify the most feasible combination of orbit and platform configuration for an ABEP mission in the 250–300 km altitude range.

E. Solar Array Arrangement vs Mean Available Power

For each of the 24 orbits listed in Table 1, we used Simulink's built-in orbit propagator [28], combined with the Sun ephemeris DE421 dataset [29], to calculate key parameters such as average eclipse duration, annual number of eclipses, and the solar vector's orientation relative to the VNB reference frame. The simulations were conducted over a one-year period, starting at UTC=0 on January 1, 2021, under the simplifying assumption of drag-free motion (i.e., the ABEP system is, on average, sufficient to counteract atmospheric drag).

As a reference, Figure 4 provides the evolution of the solar vector with respect to the VNB reference frame (assumed to coincide with the spacecraft body axes as per proposed attitude controller logic for drag minimization) for a one-year duration propagation.

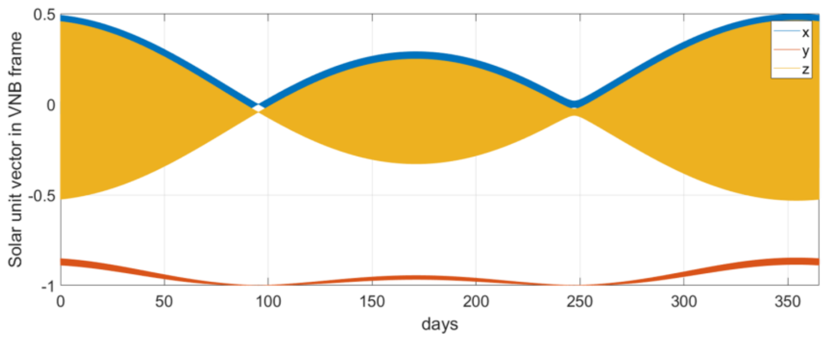

Figure 4. Evolution of solar vector wrt VNB frame for a 6am dawn-dusk orbit.

Table 5. Computed mean eclipse and solar view factors for each of the 24 orbits identified as per Table 2. Negative sign in the y view factor means that the sun vector is directed toward the east direction.

Orbit ID	α	$<T_{ecl}>$ [mm:ss]	N_{ecl} [1/yrs]	$<\boldsymbol{n_{SA,y}} \cdot \boldsymbol{n_\odot}>$	$<\boldsymbol{n_{SA,z}} \cdot \boldsymbol{n_\odot}>$	$<\boldsymbol{n_{SA,45^\circ}} \cdot \boldsymbol{n_\odot}>$
1	0.102	19:58	2685	-0.960	0.072	0.678
2	0.401	35:54	5871	-0.441	0.455	0.612
3	0.396	35:26	5871	0.520	0.429	0.648
4	0.332	33:07	5271	0.031	0.318	0.215
5	0.339	32:47	5436	0.049	0.323	0.231
6	0.331	32:16	5436	-0.068	0.303	0.230
7	0.348	33.02	5537	0.013	0.339	0.219
8	0.350	33:12	5536	0.055	0.340	0.250
9	0.338	33:00	5377	-0.051	0.319	0.231
10	0.388	34:44	5875	0.017	0.416	0.282
11	0.388	34:44	5875	0.017	0.416	0.282
12	0.384	34:23	5875	0.017	0.404	0.274
13	0.084	22:00	1993	-0.959	0.071	0.673
14	0.392	35:30	5806	-0.442	0.448	0.605
15	0.387	34:59	5806	0.519	0.422	0.639
16	0.318	32:38	5119	0.033	0.309	0.206
17	0.318	32:13	5340	0.034	0.318	0.214
18	0.316	31:16	5316	-0.057	0.297	0.213
19	0.336	32:26	5436	0.022	0.333	0.218
20	0.337	32:38	5422	0.040	0.333	0.230
21	0.324	32:19	5265	-0.049	0.311	0.219
22	0.377	34:06	5809	0.013	0.407	0.269
23	0.377	34:06	5809	0.006	0.407	0.264
24	0.376	34:00	5809	0.001	0.403	0.258

For each application orbit, Table 5 provides the computed mean eclipse to orbit period ratio , mean eclipse duration, number of eclipses per year, and mean solar view factor for a given cell with normal directed along the y, z and [0, 1/√2, 1/√2] VNB/body axes. The mean solar power available during illumination is then estimated for each combination of orbit and platform configuration by combining the data reported in Table 5 with the one of Table 3, as follows:

$$P_{av} = p_\odot (A_y < \boldsymbol{n_{SA,y}} \cdot \boldsymbol{n}_\odot > + \mathrm{A_Z} < \boldsymbol{n_{SA,z}} \cdot \boldsymbol{n}_\odot > + \mathrm{A}_{45} < \boldsymbol{n_{SA,45^\circ}} \cdot \boldsymbol{n}_\odot >) \quad (9)$$

Where $p_\odot$=250 W/m2 is the maximum generable solar power per surface area.

The resulting P_{av} is provided in Table 6. The highest power availability is achieved in 6:00 AM Sun-Synchronous Orbits (SSOs) with a platform configuration that maximizes the exposed solar cell area along the y-axis. For an Earth observation constellation, a solar array configuration tilted at 45° relative to the body axes would provide good power levels for all the investigated hours of 6:00 AM, 10:00 AM, and 2:00 PM. In contrast, inclined orbits yield the lowest power availability due to a non-negligible Sun vector component frequently aligning with the flight direction. This alignment would require reorienting the solar arrays to face the atmospheric flow directly, significantly increasing drag. Consequently, for telecommunications applications, SSOs offering global coverage are likely a more favorable choice than inclined orbits.

Table 6. Mean available solar power for each combination of orbit and platform configuration. Each row represents a platform configuration consistently with Figure 2 while each column represent an application orbit consistently with Table 2.

	Mean Available Solar Power [W]																							
Plat / Orbit	1	2	3	4	5	6	7	8	9	10	11	12	13	14	15	16	17	18	19	20	21	22	23	24
1	9.7	19.2	18.9	11.4	11.7	11.1	12.0	12.3	11.5	14.7	14.7	14.3	9.7	19.0	18.7	11.1	11.4	10.8	11.8	12.0	11.3	14.3	14.3	14.1
2	2.5	15.9	15.0	11.1	11.3	10.6	11.9	11.9	11.2	14.6	14.6	14.1	2.5	15.7	14.8	10.8	11.1	10.4	11.7	11.7	10.9	14.2	14.2	14.1
3	35.1	27.3	29.4	8.5	9.3	9.4	8.5	10.0	9.3	10.8	10.8	10.5	34.9	27.0	29.1	8.2	8.5	8.7	8.5	9.2	8.9	10.0	10.0	9.8
4	43.6	22.1	25.5	3.0	3.8	4.6	2.3	4.2	3.9	2.8	2.8	2.8	43.5	22.1	25.5	3.0	3.1	4.1	2.7	3.5	3.8	2.3	2.3	2.1
5	34.1	18.8	21.4	3.5	4.1	4.7	3.0	4.5	4.2	3.7	3.7	3.6	34.1	18.8	21.3	3.5	3.6	4.2	3.3	3.9	4.0	3.3	3.3	3.1
6	33.6	15.4	18.2	1.1	1.7	2.4	0.5	1.9	1.8	0.6	0.6	0.6	33.6	15.5	18.2	1.2	1.2	2.0	0.8	1.4	1.7	0.2	0.2	0.0
7	26.2	27.4	28.5	11.4	12.0	11.8	11.7	12.9	12.0	14.8	14.8	14.4	26.1	27.1	28.1	11.0	11.4	11.1	11.6	12.1	11.5	14.1	14.1	13.8
8	8.0	22.7	21.9	14.5	14.8	14.0	15.3	15.6	14.6	18.8	18.8	18.3	8.0	22.4	21.6	14.1	14.5	13.7	15.1	15.2	14.2	18.3	18.3	18.1
9	11.9	32.9	31.8	20.9	21.4	20.2	22.1	22.5	21.1	27.2	27.2	26.4	11.8	32.4	31.3	20.3	20.9	19.7	21.8	21.9	20.6	26.5	26.5	26.2
10	4.7	29.6	27.9	20.7	21.0	19.7	22.0	22.1	20.7	27.0	27.0	26.3	4.6	29.1	27.4	20.1	20.7	19.3	21.6	21.6	20.2	26.5	26.5	26.2
11	55.4	45.6	48.8	15.0	16.2	16.3	15.0	17.5	16.2	19.3	19.3	18.7	55.1	45.2	48.2	14.4	14.9	15.1	15.1	16.1	15.4	18.0	18.0	17.5
12	72.4	35.4	41.1	3.9	5.3	6.6	2.7	5.8	5.4	3.4	3.4	3.3	72.3	35.4	41.0	4.0	4.1	5.8	3.3	4.7	5.2	2.5	2.5	2.1
13	62.9	32.1	37.0	4.4	5.6	6.7	3.4	6.1	5.7	4.2	4.2	4.1	62.9	32.1	36.9	4.5	4.6	5.9	3.9	5.1	5.5	3.4	3.4	3.1
14	62.4	28.7	33.8	2.0	3.2	4.4	0.8	3.6	3.3	1.1	1.1	1.1	62.3	28.7	33.7	2.1	2.2	3.7	1.4	2.6	3.2	0.4	0.4	0.1
15	46.6	45.8	47.9	17.8	19.0	18.7	18.3	20.4	18.9	23.2	23.2	22.6	46.2	45.2	47.3	17.2	17.8	17.5	18.2	19.0	18.1	22.0	22.0	21.5
16	10.2	36.3	34.8	24.0	24.5	23.1	25.5	25.8	24.2	31.3	31.3	30.4	10.1	35.8	34.2	23.3	24.0	22.6	25.1	25.2	23.6	30.6	30.6	30.2
17	14.0	46.5	44.7	30.4	31.1	29.3	32.3	32.7	30.7	39.6	39.6	38.5	13.9	45.9	44.0	29.6	30.5	28.6	31.8	31.9	29.9	38.7	38.7	38.3
18	6.8	43.2	40.8	30.2	30.7	28.8	32.2	32.3	30.3	39.5	39.5	38.4	6.7	42.6	40.1	29.4	30.2	28.2	31.6	31.6	29.5	38.7	38.7	38.3
19	75.8	64.0	68.3	21.4	23.1	23.2	21.6	25.0	23.2	27.7	27.7	26.9	75.3	63.3	67.4	20.6	21.4	21.5	21.6	23.0	22.0	25.9	25.9	25.3
20	101	48.6	56.7	4.8	6.8	8.7	3.1	7.5	7.0	3.9	3.9	3.8	101	48.7	56.6	5.0	5.2	7.5	4.0	5.9	6.7	2.7	2.7	2.1
21	91.7	45.3	52.6	5.3	7.1	8.7	3.8	7.8	7.2	4.7	4.7	4.6	91.6	45.4	52.5	5.5	5.6	7.6	4.6	6.3	7.0	3.6	3.6	3.1
22	91.2	41.9	49.4	2.9	4.7	6.5	1.2	5.2	4.8	1.6	1.6	1.6	91.1	42.0	49.3	3.1	3.2	5.4	2.1	3.8	4.7	0.6	0.6	0.1
23	66.9	64.1	67.4	24.3	25.9	25.6	24.9	27.9	25.8	31.7	31.7	30.8	66.4	63.4	66.4	23.3	24.2	23.9	24.7	25.9	24.6	29.9	29.9	29.3
24	12.4	50.0	47.6	33.5	34.2	32.2	35.7	36.0	33.8	43.8	43.8	42.5	12.3	49.3	46.9	32.6	33.6	31.5	35.1	35.2	32.9	42.8	42.8	42.3

F. Platform Configuration vs Mean Atmospheric Drag and Torque

The residual aerodynamic drag and torque is estimated for each platform / orbit combination by making use of the NRLMSISE-00 [30] reference atmospheric database coupled with the recently developed ADBSat suite [31]. ADBSat is a software based on a novel implementation of a panel method which is capable of determining the aerodynamic properties of bodies in free molecular flow. The full spacecraft geometry of each configuration, inclusive of both the platform 6U body and the solar arrays, was imported in the ADBSat software. Consistently with the validation approach presented in [32], we employed the Sentman GSI model with a wall accommodation coefficient $\alpha_w = 0.9$ and a wall temperature $T_w = 300$ K, and set the 81-day average F10.7 to 138.1, the daily F10.7 to 121.7, and the Ap magnetic indices to 4. Accordingly, the aerodynamic drag in nominal attitude is computed as follows:

$$D = \frac{1}{2} C_{D,x} A_f \rho_\infty u_\infty^2 \tag{10}$$

where $C_{D,x}$ is the force coefficient as computed by ADBSat along the x flight direction / body axis. Similarly, the residual aerodynamic torque is estimated as

$$\boldsymbol{M} = \frac{1}{2} \boldsymbol{C_{\mathrm{M}}} A_f L_{S/C} \rho_\infty u_\infty^2 \tag{11}$$

where the three torque coefficients $C_{\mathrm{M}} = [C_{\mathrm{M,x}}, C_{\mathrm{M,y}}, C_{\mathrm{M,z}}]$ are an output of the ADBSat simulations. The resulting drag and torque absolute value are reported in Table 7 and Table 8, respectively, for each orbit/ platform configuration.

Table 7. Mean aerodynamic drag in μN for each combination of orbit and platform configuration.

	Mean Drag D [uN]																							
Plat / Orbit	1	2	3	4	5	6	7	8	9	10	11	12	13	14	15	16	17	18	19	20	21	22	23	24
1	232	232	232	232	232	232	232	232	232	232	232	232	84	84	84	84	84	84	84	84	84	84	84	84
2	232	232	232	232	232	232	232	232	232	232	232	232	84	84	84	84	84	84	84	84	84	84	84	84
3	231	231	231	231	231	231	231	231	231	231	231	231	84	84	84	84	84	84	84	84	84	84	84	84
4	232	232	232	232	232	232	232	232	232	232	232	232	84	84	84	84	84	84	84	84	84	84	84	84
5	232	232	232	232	232	232	232	232	232	232	232	232	84	84	84	84	84	84	84	84	84	84	84	84
6	232	232	232	232	232	232	232	232	232	232	232	232	84	84	84	84	84	84	84	84	84	84	84	84
7	231	231	231	231	231	231	231	231	231	231	231	231	84	84	84	84	84	84	84	84	84	84	84	84
8	232	232	232	232	232	232	232	232	232	232	232	232	84	84	84	84	84	84	84	84	84	84	84	84
9	270	270	270	270	270	270	270	270	270	270	270	270	98	98	98	98	98	98	98	98	98	98	98	98
10	270	270	270	270	270	270	270	270	270	270	270	270	98	98	98	98	98	98	98	98	98	98	98	98
11	267	267	267	267	267	267	267	267	267	267	267	267	97	97	97	97	97	97	97	97	97	97	97	97
12	269	269	269	269	269	269	269	269	269	269	269	269	98	98	98	98	98	98	98	98	98	98	98	98
13	270	270	270	270	270	270	270	270	270	270	270	270	98	98	98	98	98	98	98	98	98	98	98	98
14	270	270	270	270	270	270	270	270	270	270	270	270	98	98	98	98	98	98	98	98	98	98	98	98
15	267	267	267	267	267	267	267	267	267	267	267	267	97	97	97	97	97	97	97	97	97	97	97	97
16	269	269	269	269	269	269	269	269	269	269	269	269	98	98	98	98	98	98	98	98	98	98	98	98
17	307	307	307	307	307	307	307	307	307	307	307	307	112	112	112	112	112	112	112	112	112	112	112	112
18	307	307	307	307	307	307	307	307	307	307	307	307	112	112	112	112	112	112	112	112	112	112	112	112
19	303	303	303	303	303	303	303	303	303	303	303	303	111	111	111	111	111	111	111	111	111	111	111	111
20	307	307	307	307	307	307	307	307	307	307	307	307	112	112	112	112	112	112	112	112	112	112	112	112
21	307	307	307	307	307	307	307	307	307	307	307	307	112	112	112	112	112	112	112	112	112	112	112	112
22	307	307	307	307	307	307	307	307	307	307	307	307	112	112	112	112	112	112	112	112	112	112	112	112
23	303	303	303	303	303	303	303	303	303	303	303	303	111	111	111	111	111	111	111	111	111	111	111	111
24	307	307	307	307	307	307	307	307	307	307	307	307	112	112	112	112	112	112	112	112	112	112	112	112

Table 8. Mean aerodynamic torque in μNm for each combination of orbit and platform configuration.

	Mean Torque M [uNm]																							
Plat / Orbit	1	2	3	4	5	6	7	8	9	10	11	12	13	14	15	16	17	18	19	20	21	22	23	24
1	0.00	0.00	0.00	0.00	0.00	0.00	0.00	0.00	0.00	0.00	0.00	0.00	0.00	0.00	0.00	0.00	0.00	0.00	0.00	0.00	0.00	0.00	0.00	0.00
2	4.69	4.69	4.69	4.69	4.69	4.69	4.69	4.69	4.69	4.69	4.69	4.69	1.77	1.77	1.77	1.77	1.77	1.77	1.77	1.77	1.77	1.77	1.77	1.77
3	0.05	0.05	0.05	0.05	0.05	0.05	0.05	0.05	0.05	0.05	0.05	0.05	0.02	0.02	0.02	0.02	0.02	0.02	0.02	0.02	0.02	0.02	0.02	0.02
4	0.12	0.12	0.12	0.12	0.12	0.12	0.12	0.12	0.12	0.12	0.12	0.12	0.05	0.05	0.05	0.05	0.05	0.05	0.05	0.05	0.05	0.05	0.05	0.05
5	0.00	0.00	0.00	0.00	0.00	0.00	0.00	0.00	0.00	0.00	0.00	0.00	0.00	0.00	0.00	0.00	0.00	0.00	0.00	0.00	0.00	0.00	0.00	0.00
6	4.69	4.69	4.69	4.69	4.69	4.69	4.69	4.69	4.69	4.69	4.69	4.69	1.77	1.77	1.77	1.77	1.77	1.77	1.77	1.77	1.77	1.77	1.77	1.77
7	0.05	0.05	0.05	0.05	0.05	0.05	0.05	0.05	0.05	0.05	0.05	0.05	0.02	0.02	0.02	0.02	0.02	0.02	0.02	0.02	0.02	0.02	0.02	0.02
8	0.12	0.12	0.12	0.12	0.12	0.12	0.12	0.12	0.12	0.12	0.12	0.12	0.05	0.05	0.05	0.05	0.05	0.05	0.05	0.05	0.05	0.05	0.05	0.05
9	0.00	0.00	0.00	0.00	0.00	0.00	0.00	0.00	0.00	0.00	0.00	0.00	0.00	0.00	0.00	0.00	0.00	0.00	0.00	0.00	0.00	0.00	0.00	0.00
10	9.37	9.37	9.37	9.37	9.37	9.37	9.37	9.37	9.37	9.37	9.37	9.37	3.53	3.53	3.53	3.53	3.53	3.53	3.53	3.53	3.53	3.53	3.53	3.53
11	0.09	0.09	0.09	0.09	0.09	0.09	0.09	0.09	0.09	0.09	0.09	0.09	0.04	0.04	0.04	0.04	0.04	0.04	0.04	0.04	0.04	0.04	0.04	0.04
12	0.25	0.25	0.25	0.25	0.25	0.25	0.25	0.25	0.25	0.25	0.25	0.25	0.09	0.09	0.09	0.09	0.09	0.09	0.09	0.09	0.09	0.09	0.09	0.09
13	0.00	0.00	0.00	0.00	0.00	0.00	0.00	0.00	0.00	0.00	0.00	0.00	0.00	0.00	0.00	0.00	0.00	0.00	0.00	0.00	0.00	0.00	0.00	0.00
14	9.37	9.37	9.37	9.37	9.37	9.37	9.37	9.37	9.37	9.37	9.37	9.37	3.53	3.53	3.53	3.53	3.53	3.53	3.53	3.53	3.53	3.53	3.53	3.53
15	0.09	0.09	0.09	0.09	0.09	0.09	0.09	0.09	0.09	0.09	0.09	0.09	0.04	0.04	0.04	0.04	0.04	0.04	0.04	0.04	0.04	0.04	0.04	0.04
16	0.25	0.25	0.25	0.25	0.25	0.25	0.25	0.25	0.25	0.25	0.25	0.25	0.09	0.09	0.09	0.09	0.09	0.09	0.09	0.09	0.09	0.09	0.09	0.09
17	0.00	0.00	0.00	0.00	0.00	0.00	0.00	0.00	0.00	0.00	0.00	0.00	0.00	0.00	0.00	0.00	0.00	0.00	0.00	0.00	0.00	0.00	0.00	0.00
18	14.1	14.1	14.1	14.1	14.1	14.1	14.1	14.1	14.1	14.1	14.1	14.1	5.30	5.30	5.30	5.30	5.30	5.30	5.30	5.30	5.30	5.30	5.30	5.30
19	0.14	0.14	0.14	0.14	0.14	0.14	0.14	0.14	0.14	0.14	0.14	0.14	0.06	0.06	0.06	0.06	0.06	0.06	0.06	0.06	0.06	0.06	0.06	0.06
20	0.37	0.37	0.37	0.37	0.37	0.37	0.37	0.37	0.37	0.37	0.37	0.37	0.14	0.14	0.14	0.14	0.14	0.14	0.14	0.14	0.14	0.14	0.14	0.14
21	0.00	0.00	0.00	0.00	0.00	0.00	0.00	0.00	0.00	0.00	0.00	0.00	0.00	0.00	0.00	0.00	0.00	0.00	0.00	0.00	0.00	0.00	0.00	0.00
22	14.1	14.1	14.1	14.1	14.1	14.1	14.1	14.1	14.1	14.1	14.1	14.1	5.30	5.30	5.30	5.30	5.30	5.30	5.30	5.30	5.30	5.30	5.30	5.30
23	0.14	0.14	0.14	0.14	0.14	0.14	0.14	0.14	0.14	0.14	0.14	0.14	0.06	0.06	0.06	0.06	0.06	0.06	0.06	0.06	0.06	0.06	0.06	0.06
24	0.37	0.37	0.37	0.37	0.37	0.37	0.37	0.37	0.37	0.37	0.37	0.37	0.14	0.14	0.14	0.14	0.14	0.14	0.14	0.14	0.14	0.14	0.14	0.14

As indicated in Table 8, an asymmetric platform geometry increases the residual aerodynamic torque. Considering an average 25 μT value for Earth's magnetic field intensity, the selected magnetorquers (having a maximum dipole moment of approximately 0.3 Am² per axis [21]), can apply a peak desaturating torque of about 7.5 μNm. Consequently, configurations #10, #14, #18, and #22 appear impractical at 250 km of altitude due to the likelihood of reaction wheel saturation and attitude control failure. Moreover, given the significant uncertainties associated with a more detailed spacecraft geometry and space weather conditions, configurations #1,#5,#9,#13,#17, and #21, which minimize aerodynamic torque, shall be strongly preferred from an attitude stability perspective.

III. Tradeoffs Results and Comparison with Conventional Propulsion

A. Air-breathing vs conventional Propulsion Efficiency Requirement

Tables 1 and 2 summarize the efficiency requirements as derived in Section II for conventional propulsion and ABEP, respectively. For the conventional case, the efficiency is evaluated assuming a propulsion system with a specific impulse of 2000 s, noting that lower specific impulse values would further reduce the minimum efficiency requirement at the expense of a likely reduced total impulse capability of the system.

Across all considered orbit–platform combinations, the efficiency requirement for conventional propulsion is consistently less than the corresponding ABEP requirement. This discrepancy arises because the atmospheric flow in VLEO is characterized by both low mass flow rates and low molecular mass, in contrast to systems relying on on-board propellant, which typically provide higher mass flow rates with propellants of greater molecular mass. Consequently, in order to compensate for the same level of drag, ABEP systems must operate at significantly higher specific impulse, which in turn demands higher power for an equivalent thrust level. Therefore, under conditions where the available power for propulsion is constrained, ABEP must achieve substantially higher efficiency to remain viable. From a feasibility perspective, this highlights the greater technological challenge of ABEP compared to conventional propulsion counterparts. Concerning the feasibility of mission scenarios based on ABEP nanosatellites, the following considerations can be made based on the trade-off result:

- **Minimum Efficiency**: The minimum efficiency requirement is obtained for the platform configuration #20, which maximize the solar array area exposed along the y-axis, and the dawn-dusk SSO orbits, which offers the best illumination conditions. The resulting minimum efficiency equals $\eta_c\eta_T \geq 10.4\%$ at 250 km of altitude, which reduces to $\eta_c\eta_T \geq 3.8\%$ at 300 km.
- **Feasible Configurations for Constellations**: Platform configurations #19 and #23, in conjunction with an ABEP efficiency of $\eta_c\eta_T \geq 10\%$, would enable the deployment of a feasible spacecraft constellation in 300 km SSO orbits distributed across various RAANs.
- **Aerodynamic Torque Reduction**: For platform configuration #21, which minimizes residual aerodynamic torque with minimum impact on the power generation capabilities, an ABEP efficiency of $\eta_c\eta_T \geq 11.7\%$ is required for dawn-dusk SSO operations at 250 km altitude. This requirement reduces to $\eta_c\eta_T \geq 4.2\%$ at 300 km altitude.
- **Cost reduction:** For platform configuration #13, another option minimizing aerodynamic torque but requiring only 2-folds solar arrays, an efficiency of $\eta_c\eta_T \geq 13.8\%$ would be needed at 250 km altitude, decreasing to $\eta_c\eta_T \geq 5.0\%$ at 300 km.

Table 9. Conventional EP η_T efficiency requirement for each combination of orbit and platform configuration.

	Conventional propulsion efficiency req, 2000s																							
Plat / Orbit	1	2	3	4	5	6	7	8	9	10	11	12	13	14	15	16	17	18	19	20	21	22	23	24
1	0.94	0.44	0.45	1.00	1.00	1.00	1.00	1.00	1.00	0.85	0.85	0.92	0.32	0.16	0.16	0.67	0.57	0.76	0.54	0.51	0.64	0.32	0.32	0.33
2	1.00	0.71	0.83	1.00	1.00	1.00	1.00	1.00	1.00	0.88	0.88	0.95	1.00	0.26	0.30	0.77	0.64	1.00	0.58	0.58	0.79	0.32	0.32	0.33
3	0.09	0.23	0.20	1.00	1.00	1.00	1.00	1.00	1.00	1.00	1.00	1.00	0.03	0.08	0.07	1.00	1.00	1.00	1.00	1.00	1.00	1.00	1.00	1.00
4	0.07	0.33	0.25	1.00	1.00	1.00	1.00	1.00	1.00	1.00	1.00	1.00	0.02	0.12	0.09	1.00	1.00	1.00	1.00	1.00	1.00	1.00	1.00	1.00
5	0.09	0.46	0.34	1.00	1.00	1.00	1.00	1.00	1.00	1.00	1.00	1.00	0.03	0.16	0.12	1.00	1.00	1.00	1.00	1.00	1.00	1.00	1.00	1.00
6	0.10	0.78	0.49	1.00	1.00	1.00	1.00	1.00	1.00	1.00	1.00	1.00	0.03	0.27	0.17	1.00	1.00	1.00	1.00	1.00	1.00	1.00	1.00	1.00
7	0.13	0.22	0.21	1.00	1.00	1.00	1.00	1.00	1.00	0.83	0.83	0.89	0.05	0.08	0.08	0.70	0.57	0.63	0.58	0.48	0.56	0.34	0.34	0.36
8	1.00	0.31	0.33	0.68	0.66	0.75	0.62	0.60	0.68	0.44	0.44	0.46	0.82	0.11	0.12	0.25	0.23	0.27	0.22	0.22	0.25	0.16	0.16	0.16
9	0.61	0.20	0.21	0.35	0.34	0.37	0.33	0.32	0.35	0.26	0.26	0.27	0.21	0.07	0.07	0.13	0.12	0.13	0.12	0.12	0.13	0.09	0.09	0.10
10	1.00	0.23	0.25	0.35	0.35	0.39	0.33	0.33	0.36	0.26	0.26	0.27	1.00	0.08	0.09	0.13	0.12	0.14	0.12	0.12	0.13	0.09	0.09	0.10
11	0.06	0.12	0.11	0.71	0.59	0.57	0.75	0.52	0.59	0.48	0.48	0.50	0.02	0.05	0.04	0.27	0.25	0.24	0.26	0.22	0.23	0.20	0.20	0.21
12	0.05	0.18	0.14	1.00	1.00	1.00	1.00	1.00	1.00	1.00	1.00	1.00	0.02	0.06	0.05	1.00	1.00	1.00	1.00	1.00	1.00	1.00	1.00	1.00
13	0.05	0.21	0.16	1.00	1.00	1.00	1.00	1.00	1.00	1.00	1.00	1.00	0.02	0.07	0.06	1.00	1.00	1.00	1.00	1.00	1.00	1.00	1.00	1.00
14	0.05	0.24	0.19	1.00	1.00	1.00	1.00	1.00	1.00	1.00	1.00	1.00	0.02	0.09	0.07	1.00	1.00	1.00	1.00	1.00	1.00	1.00	1.00	1.00
15	0.07	0.12	0.12	0.47	0.42	0.42	0.47	0.38	0.42	0.33	0.33	0.34	0.03	0.04	0.04	0.18	0.16	0.17	0.17	0.15	0.16	0.13	0.13	0.13
16	0.93	0.17	0.18	0.27	0.27	0.29	0.26	0.25	0.27	0.21	0.21	0.21	0.32	0.06	0.07	0.10	0.10	0.11	0.09	0.09	0.10	0.08	0.08	0.08
17	0.48	0.14	0.15	0.21	0.21	0.23	0.20	0.20	0.22	0.17	0.17	0.17	0.17	0.05	0.05	0.08	0.08	0.08	0.07	0.07	0.08	0.06	0.06	0.06
18	1.00	0.15	0.16	0.22	0.22	0.23	0.21	0.21	0.22	0.17	0.17	0.17	1.00	0.06	0.06	0.08	0.08	0.08	0.07	0.08	0.08	0.06	0.06	0.06
19	0.05	0.09	0.09	0.37	0.33	0.32	0.38	0.30	0.33	0.28	0.28	0.29	0.02	0.03	0.03	0.14	0.13	0.13	0.13	0.12	0.13	0.11	0.11	0.11
20	0.04	0.13	0.11	1.00	1.00	1.00	1.00	1.00	1.00	1.00	1.00	1.00	0.01	0.05	0.04	1.00	1.00	1.00	1.00	1.00	1.00	1.00	1.00	1.00
21	0.04	0.14	0.12	1.00	1.00	1.00	1.00	1.00	1.00	1.00	1.00	1.00	0.01	0.05	0.04	1.00	1.00	1.00	1.00	1.00	1.00	1.00	1.00	1.00
22	0.04	0.16	0.13	1.00	1.00	1.00	1.00	1.00	1.00	1.00	1.00	1.00	0.01	0.06	0.05	1.00	1.00	1.00	1.00	1.00	1.00	1.00	1.00	1.00
23	0.06	0.09	0.09	0.30	0.28	0.27	0.30	0.25	0.28	0.23	0.23	0.23	0.02	0.03	0.03	0.11	0.11	0.11	0.11	0.10	0.10	0.09	0.09	0.09
24	0.63	0.13	0.13	0.19	0.19	0.20	0.18	0.18	0.19	0.15	0.15	0.15	0.22	0.05	0.05	0.07	0.07	0.07	0.06	0.06	0.07	0.05	0.05	0.05

Table 10. $\eta_c \eta_T$ efficiency requirement for each combination of orbit and platform configuration for an intake area of 0.01 m^2

	ABEP eta_C*eta_T requirement																							
Plat / Orbit	1	2	3	4	5	6	7	8	9	10	11	12	13	14	15	16	17	18	19	20	21	22	23	24
1	1.00	1.00	1.00	1.00	1.00	1.00	1.00	1.00	1.00	1.00	1.00	1.00	1.00	0.54	0.56	1.00	1.00	1.00	1.00	1.00	1.00	1.00	1.00	1.00
2	1.00	1.00	1.00	1.00	1.00	1.00	1.00	1.00	1.00	1.00	1.00	1.00	1.00	1.00	1.00	1.00	1.00	1.00	1.00	1.00	1.00	1.00	1.00	1.00
3	0.21	0.60	0.51	1.00	1.00	1.00	1.00	1.00	1.00	1.00	1.00	1.00	0.08	0.22	0.19	1.00	1.00	1.00	1.00	1.00	1.00	1.00	1.00	1.00
4	0.16	0.97	0.68	1.00	1.00	1.00	1.00	1.00	1.00	1.00	1.00	1.00	0.06	0.34	0.24	1.00	1.00	1.00	1.00	1.00	1.00	1.00	1.00	1.00
5	0.22	1.00	1.00	1.00	1.00	1.00	1.00	1.00	1.00	1.00	1.00	1.00	0.08	0.56	0.37	1.00	1.00	1.00	1.00	1.00	1.00	1.00	1.00	1.00
6	0.22	1.00	1.00	1.00	1.00	1.00	1.00	1.00	1.00	1.00	1.00	1.00	0.08	1.00	0.62	1.00	1.00	1.00	1.00	1.00	1.00	1.00	1.00	1.00
7	0.32	0.59	0.54	1.00	1.00	1.00	1.00	1.00	1.00	1.00	1.00	1.00	0.11	0.22	0.20	1.00	1.00	1.00	1.00	1.00	1.00	1.00	1.00	1.00
8	1.00	0.91	0.98	1.00	1.00	1.00	1.00	1.00	1.00	1.00	1.00	1.00	1.00	0.33	0.36	1.00	1.00	1.00	0.99	0.97	1.00	0.56	0.56	0.58
9	1.00	0.58	0.61	1.00	1.00	1.00	1.00	1.00	1.00	0.79	0.79	0.83	0.95	0.21	0.22	0.44	0.41	0.47	0.39	0.39	0.43	0.30	0.30	0.30
10	1.00	0.70	0.77	1.00	1.00	1.00	1.00	1.00	1.00	0.80	0.80	0.84	1.00	0.26	0.29	0.45	0.42	0.49	0.40	0.40	0.45	0.30	0.30	0.30
11	0.16	0.34	0.31	1.00	1.00	1.00	1.00	1.00	1.00	1.00	1.00	1.00	0.06	0.13	0.11	1.00	1.00	1.00	1.00	0.99	1.00	0.81	0.81	0.89
12	0.12	0.51	0.40	1.00	1.00	1.00	1.00	1.00	1.00	1.00	1.00	1.00	0.04	0.18	0.15	1.00	1.00	1.00	1.00	1.00	1.00	1.00	1.00	1.00
13	0.14	0.61	0.47	1.00	1.00	1.00	1.00	1.00	1.00	1.00	1.00	1.00	0.05	0.22	0.17	1.00	1.00	1.00	1.00	1.00	1.00	1.00	1.00	1.00
14	0.14	0.74	0.55	1.00	1.00	1.00	1.00	1.00	1.00	1.00	1.00	1.00	0.05	0.27	0.20	1.00	1.00	1.00	1.00	1.00	1.00	1.00	1.00	1.00
15	0.19	0.34	0.31	1.00	1.00	1.00	1.00	1.00	1.00	1.00	1.00	1.00	0.07	0.13	0.12	0.69	0.62	0.64	0.62	0.55	0.60	0.44	0.44	0.46
16	1.00	0.49	0.52	0.85	0.83	0.92	0.79	0.78	0.85	0.61	0.61	0.63	1.00	0.18	0.19	0.32	0.30	0.34	0.29	0.29	0.32	0.23	0.23	0.23
17	1.00	0.44	0.46	0.71	0.70	0.76	0.67	0.66	0.71	0.54	0.54	0.56	0.71	0.16	0.17	0.27	0.26	0.28	0.25	0.25	0.27	0.20	0.20	0.21
18	1.00	0.49	0.53	0.72	0.72	0.78	0.68	0.68	0.73	0.54	0.54	0.56	1.00	0.18	0.20	0.27	0.26	0.29	0.25	0.25	0.27	0.20	0.20	0.21
19	0.14	0.28	0.25	1.00	1.00	1.00	1.00	1.00	1.00	0.96	0.96	1.00	0.05	0.10	0.09	0.54	0.49	0.48	0.51	0.45	0.47	0.40	0.40	0.41
20	0.10	0.41	0.33	1.00	1.00	1.00	1.00	1.00	1.00	1.00	1.00	1.00	0.04	0.15	0.12	1.00	1.00	1.00	1.00	1.00	1.00	1.00	1.00	1.00
21	0.12	0.46	0.37	1.00	1.00	1.00	1.00	1.00	1.00	1.00	1.00	1.00	0.04	0.17	0.13	1.00	1.00	1.00	1.00	1.00	1.00	1.00	1.00	1.00
22	0.12	0.51	0.40	1.00	1.00	1.00	1.00	1.00	1.00	1.00	1.00	1.00	0.04	0.19	0.15	1.00	1.00	1.00	1.00	1.00	1.00	1.00	1.00	1.00
23	0.16	0.28	0.26	1.00	0.94	0.94	1.00	0.85	0.94	0.75	0.75	0.78	0.06	0.10	0.10	0.41	0.38	0.38	0.38	0.35	0.37	0.30	0.30	0.31
24	1.00	0.40	0.42	0.61	0.60	0.65	0.57	0.57	0.61	0.46	0.46	0.48	1.00	0.15	0.16	0.23	0.22	0.24	0.21	0.21	0.23	0.17	0.17	0.18

B. Air-breathing vs conventional Propulsion Total Impulse

Although ABEP is more technologically demanding, particularly in terms of the efficiency requirements discussed in the previous section, it offers the key advantage of potentially extending the lifetime of VLEO platforms, since the system is no longer constrained by the finite amount of on-board propellant. However, long-term compatibility of the device with the VLEO environment remains a critical challenge. To quantify the requirements, Table 2 reports the annual total impulse that a propulsion system must deliver, for each investigated platform and orbit configuration, in order to fully compensate for atmospheric drag.

Table 11. kNs of total impulse per year needed to compensate for drag for each combination of orbit and platform configurations

	Total impulse per year [kNs/yr] needed for drag compensation																							
Plat / Orbit	1	2	3	4	5	6	7	8	9	10	11	12	13	14	15	16	17	18	19	20	21	22	23	24
1	7.33	7.33	7.33	7.33	7.33	7.33	7.33	7.33	7.33	7.33	7.33	7.33	2.66	2.66	2.66	2.66	2.66	2.66	2.66	2.66	2.66	2.66	2.66	2.66
2	7.33	7.33	7.33	7.33	7.33	7.33	7.33	7.33	7.33	7.33	7.33	7.33	2.66	2.66	2.66	2.66	2.66	2.66	2.66	2.66	2.66	2.66	2.66	2.66
3	7.28	7.28	7.28	7.28	7.28	7.28	7.28	7.28	7.28	7.28	7.28	7.28	2.64	2.64	2.64	2.64	2.64	2.64	2.64	2.64	2.64	2.64	2.64	2.64
4	7.31	7.31	7.31	7.31	7.31	7.31	7.31	7.31	7.31	7.31	7.31	7.31	2.65	2.65	2.65	2.65	2.65	2.65	2.65	2.65	2.65	2.65	2.65	2.65
5	7.33	7.33	7.33	7.33	7.33	7.33	7.33	7.33	7.33	7.33	7.33	7.33	2.66	2.66	2.66	2.66	2.66	2.66	2.66	2.66	2.66	2.66	2.66	2.66
6	7.33	7.33	7.33	7.33	7.33	7.33	7.33	7.33	7.33	7.33	7.33	7.33	2.66	2.66	2.66	2.66	2.66	2.66	2.66	2.66	2.66	2.66	2.66	2.66
7	7.28	7.28	7.28	7.28	7.28	7.28	7.28	7.28	7.28	7.28	7.28	7.28	2.64	2.64	2.64	2.64	2.64	2.64	2.64	2.64	2.64	2.64	2.64	2.64
8	7.31	7.31	7.31	7.31	7.31	7.31	7.31	7.31	7.31	7.31	7.31	7.31	2.65	2.65	2.65	2.65	2.65	2.65	2.65	2.65	2.65	2.65	2.65	2.65
9	8.51	8.51	8.51	8.51	8.51	8.51	8.51	8.51	8.51	8.51	8.51	8.51	3.10	3.10	3.10	3.10	3.10	3.10	3.10	3.10	3.10	3.10	3.10	3.10
10	8.51	8.51	8.51	8.51	8.51	8.51	8.51	8.51	8.51	8.51	8.51	8.51	3.10	3.10	3.10	3.10	3.10	3.10	3.10	3.10	3.10	3.10	3.10	3.10
11	8.43	8.43	8.43	8.43	8.43	8.43	8.43	8.43	8.43	8.43	8.43	8.43	3.07	3.07	3.07	3.07	3.07	3.07	3.07	3.07	3.07	3.07	3.07	3.07
12	8.50	8.50	8.50	8.50	8.50	8.50	8.50	8.50	8.50	8.50	8.50	8.50	3.09	3.09	3.09	3.09	3.09	3.09	3.09	3.09	3.09	3.09	3.09	3.09
13	8.51	8.51	8.51	8.51	8.51	8.51	8.51	8.51	8.51	8.51	8.51	8.51	3.10	3.10	3.10	3.10	3.10	3.10	3.10	3.10	3.10	3.10	3.10	3.10
14	8.51	8.51	8.51	8.51	8.51	8.51	8.51	8.51	8.51	8.51	8.51	8.51	3.10	3.10	3.10	3.10	3.10	3.10	3.10	3.10	3.10	3.10	3.10	3.10
15	8.43	8.43	8.43	8.43	8.43	8.43	8.43	8.43	8.43	8.43	8.43	8.43	3.07	3.07	3.07	3.07	3.07	3.07	3.07	3.07	3.07	3.07	3.07	3.07
16	8.50	8.50	8.50	8.50	8.50	8.50	8.50	8.50	8.50	8.50	8.50	8.50	3.09	3.09	3.09	3.09	3.09	3.09	3.09	3.09	3.09	3.09	3.09	3.09
17	9.70	9.70	9.70	9.70	9.70	9.70	9.70	9.70	9.70	9.70	9.70	9.70	3.54	3.54	3.54	3.54	3.54	3.54	3.54	3.54	3.54	3.54	3.54	3.54
18	9.70	9.70	9.70	9.70	9.70	9.70	9.70	9.70	9.70	9.70	9.70	9.70	3.54	3.54	3.54	3.54	3.54	3.54	3.54	3.54	3.54	3.54	3.54	3.54
19	9.55	9.55	9.55	9.55	9.55	9.55	9.55	9.55	9.55	9.55	9.55	9.55	3.49	3.49	3.49	3.49	3.49	3.49	3.49	3.49	3.49	3.49	3.49	3.49
20	9.68	9.68	9.68	9.68	9.68	9.68	9.68	9.68	9.68	9.68	9.68	9.68	3.54	3.54	3.54	3.54	3.54	3.54	3.54	3.54	3.54	3.54	3.54	3.54
21	9.70	9.70	9.70	9.70	9.70	9.70	9.70	9.70	9.70	9.70	9.70	9.70	3.54	3.54	3.54	3.54	3.54	3.54	3.54	3.54	3.54	3.54	3.54	3.54
22	9.70	9.70	9.70	9.70	9.70	9.70	9.70	9.70	9.70	9.70	9.70	9.70	3.54	3.54	3.54	3.54	3.54	3.54	3.54	3.54	3.54	3.54	3.54	3.54
23	9.55	9.55	9.55	9.55	9.55	9.55	9.55	9.55	9.55	9.55	9.55	9.55	3.49	3.49	3.49	3.49	3.49	3.49	3.49	3.49	3.49	3.49	3.49	3.49
24	9.68	9.68	9.68	9.68	9.68	9.68	9.68	9.68	9.68	9.68	9.68	9.68	3.54	3.54	3.54	3.54	3.54	3.54	3.54	3.54	3.54	3.54	3.54	3.54

With respect to propulsion performance, total impulse represents the product of the propellant mass M_p stored onboard and the thruster's specific impulse I_{sp} scaled by standard gravity g_0, such as $I = M_p I_{sp} g_0$. Accordingly, a requirement on total impulse places critical constraints on propulsion system design, influencing choices related to the acceleration mechanism, propellant storage capacity, system envelope, and overall propulsion subsystem budgets (including power since, for electric thrusters, achieving higher specific impulse at a given thrust and efficiency level demands increased power). In this regard, Table 12 lists the declared total impulse capability of several existing COTS CubeSat electric propulsion systems, and compares them with the minimum operational lifetime that an ABEP system must demonstrate in order to exceed the performance of current conventional solutions.

Table 12. COTS propulsion systems for CubeSat specifications and mission lifetime expectancy in VLEO.

Propulsion System	Tech. / propellant	Volume [U]	Thrust [mN]	Power [W]	Total Impulse [kNs]	High-power 6U lifetime at 250 km [months]	High-power 6U lifetime at 300 km [months]
SpaceWare Nano	HET Xenon	2.5	<2.5	60	6	7.4	20.3
Regulus-50	IPT Iodine	1.5	<0.65	30 to 60	3	3.7	10.2
Nano Lark	FEEP Indium	1	<0.35	15 to 45	4	4.9	13.6
NPT30-I2	RIT Iodine	1	<1.1	35-65	5.5	6.8	18.6
BIT3-I2	RIT Iodine	2	<1.1	56 to 75	12.3*	15.2	41.6

*12.3 kNs demonstrated according to [38], ≈30 kNs according to online datasheet.

IV.Conclusions

In this work, a reference 6U CubeSat was considered for VLEO applications, and a set of trade-offs was performed to assess the feasibility requirements for extended missions in the 250–300 km altitude range, comparing conventional and air-breathing propulsion systems. A total of 24 orbit scenarios and 24 CubeSat configurations were investigated, from which orbit-averaged representative values of aerodynamic drag and mean solar power availability were derived. Using a set of reference COTS payloads and CubeSat subsystems, a preliminary power budget was established, which provided the propulsion power allocation for each configuration. This allowed determination of the propulsion efficiency required to perform drag compensation while remaining within platform power limits for both conventional and ABEP systems. The results indicated that efficiency requirements were generally more stringent for ABEP. Nevertheless, conventional propellant-based systems with current technology could typically achieve mission lifetimes of only a few months at 250 km, highlighting the potential of ABEP to enable extended VLEO operations.

Acknowledgments

This work was supported by the Italian Ministry of University and Research (MUR) under the FISA-2022-00887 project *ARIA Air-breathing Rocket for Innovative Applications,* Unique Project Code (CUP) J53C24000390001. The views and opinions expressed are those of the authors and do not necessarily reflect those of the funding institution.

References

1. Berthoud, L., et al., "Are very low earth orbit (vleo) satellites a solution for tomorrow's telecommunication needs?". CEAS Space Journal, Volume 14, pages 609–623, 2022
2. N.H. Crisp, P.C. Roberts, F. Romano, K.L. Smith, V.T. Oiko, V. Sulliotti-Linner, V. Hanessian, G.H. Herdrich, D. García-Almiñana, D. Kataria, S. Seminari, System modelling of very low earth orbit satellites for earth observation, Acta Astronaut. 187 (June) (2021) 475–491, http://dx.doi.org/10.1016/j.actaastro.2021.07.004.
3. C. McGrath, C. Lowe, M. Macdonald, S. Hancock, Investigation of very low earth orbits (VLEOs) for global spaceborne lidar, CEAS Space J. (0123456789) (2022) http://dx.doi.org/10.1007/s12567-022-00427-2.
4. L.M.S. Martines, Analysis of LEO Radiation Environment and its Effects on Spacecraft's Critical Electronic Devices (Ph.D. thesis), Embry-Riddle Aeronautical University, 2011, URL: https://commons.erau.edu/edt/102.
5. P.C.E. Roberts, "1st Symposium of Very Low Earth Orbit Missions and Technologies". CEAS Space Journal, Volume 14, pages 605–608, 2022
6. V. Giannetti, E. Ferrato, and T. Andreussi, "On the critical parameters for feasibility and advantage of air-breathing electric propulsion systems," Acta Astronautica, vol. 220, pp. 345–355, 2024.
7. T. Andreussi, E. Ferrato, and V. Giannetti (2022), "A review of air-breathing electric propulsion: from mission studies to technology verification", Journal of Electric Propulsion 1 (31)
8. E. Ferrato, V. Giannetti, and T. Andreussi, "Guidance, Navigation, and Control of a Low-Altitude Nanosatellite equipped with Air-breathing Electric Propulsion", IEEE Transactions on Aerospace and Electronic Systems, doi:10.1109/TAES.2025.3577159
9. M. Tisaev, E. Ferrato, V. Giannetti, C. Paissoni, N. Baresi, A. Lucca Fabris, and T. Andreussi, "Air-breathing electric propulsion: Flight envelope identification and development of control for long-term orbital stability," Acta Astronautica, vol. 191, no. October 2021, pp. 374–393, 2022.
10. N. Pachler et al., "An Updated Comparison of Four Low Earth Orbit Satellite Constellation Systems to Provide Global Broadband," 2021 IEEE International Conference on Communications Workshops (ICC Workshops), Montreal, QC, Canada, 2021, pp. 1-7, doi: 10.1109/ICCWorkshops50388.2021.9473799.
11. https://earth.esa.int/eogateway/missions/planetscope, accessed on 1st Sep 2025
12. https://earth.esa.int/eogateway/missions/iceye, accessed on 1st Sep 2025
13. https://earth.esa.int/eogateway/missions/worldview-3, accessed on 1st Sep 2025
14. https://gomspace.com/shop/subsystems/power/nanopower-tsp.aspx, accessed on 1st Sep 2025
15. GomSpace website, https://gomspace.com/home.aspx, accessed on 1st Sep 2025
16. https://simera-sense.com/products/triscape100/, accessed on 1st Sep 2025
17. https://gomspace.com/shop/subsystems/power/nanopower-tsp.aspx, accessed on 1st Sep 2025
18. https://gomspace.com/shop/subsystems/power/nanopower-bpx.aspx, accessed on 1st Sep 2025
19. https://gomspace.com/shop/subsystems/power/nanopower-p60.aspx, accessed on 1st Sep 2025
20. https://gomspace.com/shop/subsystems/attitude-orbit-control-systems/nanotorque-gsw-600.aspx, accessed on 1st Sep 2025
21. https://gomspace.com/shop/subsystems/attitude-orbit-control-systems/nanotorque-gst-600.aspx, accessed on 1st Sep 2025
22. https://www.arcsec.space/twinkle/, accessed on 1st Sep 2025
23. https://gomspace.com/shop/subsystems/attitude-orbit-control-systems/nanosense-m315.aspx, accessed on 1st Sep 2025
24. https://novatel.com/products/receivers/gnss-gps-receiver-boards/oem719, accessed on 1st Sep 2025
25. https://gomspace.com/shop/subsystems/command-and-data-handling/nanomind-hp-mk3-(1).aspx, accessed on 1st Sep 2025
26. https://gomspace.com/shop/subsystems/communication-systems/nanocom-link-s.aspx, accessed on 1st Sep 2025
27. https://gomspace.com/shop/subsystems/communication-systems/nanocom-ant2000.aspx, accessed on 1st Sep 2025
28. https://it.mathworks.com/help/aeroblks/spacecraftdynamics.html, accessed on 1st Sep 2025
29. W. M. Folkner, J. G. Williams, and D. H. Boggs, "The Planetary and Lunar Ephemeris DE 421," IPN Progress Report 42–178, 2009.
30. J. Picone, et al., "NRLMSISE-00 empirical model of the atmosphere: Statistical comparisons and scientific issues," Journal of Geophysical Research, vol. 107, no. A12, p. 1468, 2002.
31. L. A. Sinpetru, et al., ADBSat: Methodology of a novel panel method tool for aerodynamic analysis of satellites, Computer Physics Communications, vol. 275, 2022.
32. L. A. Sinpetru, et al., ADBSat: Verification and validation of a novel panel method for quick aerodynamic analysis of satellites, Computer Physics Communications, Vol. 275, 2022.

33. https://www.exotrail.com/product/spaceware, accessed on 1st Sep 2025
34. https://www.t4innovation.com/regulus-50-electric-propulsion-system/, accessed on 1st Sep 2025
35. https://www.enpulsion.com/propulsion/, accessed on 1st Sep 2025
36. https://www.thrustme.fr/products/npt30-i2, accessed on 1st Sep 2025
37. https://www.busek.com/bit3, accessed on 1st Sep 2025
38. Michael Tsay, Riley Terhaar, Kyle Emmi and Carl Barcroft, "Twin Ion Engine Demonstration for Small Spacecraft Applications", 36th Annual Small Satellite Conference, Logan, UT, 2022.